CORRECTION OF OFFSET IN MDI/SOHO MAGNETOGRAMS

YANG LIU, XUEPU ZHAO and J. TODD HOEKSEMA
W. W. Hansen Experimental Physics Laboratory, Stanford University, Stanford, CA 94305-4085, U.S.A. (e-mail: yliu@quake.stanford.edu)

(Received 11 April 2003; accepted 4 November 2003)

Abstract. Shutter noise induces a small random shift of the zero point in full-disk magnetograms obtained by the Michelson Doppler Imager (MDI) instrument aboard SOHO. In this paper, we develop a method to remove this offset by fitting the distribution of the magnetic field strength with a Gaussian function (Ulrich *et al.*, 2002). We also discover a systematic error in the five-minute magnetograms that are the sum of five individual magnetograms computed on-board; this error can be removed together with the offset. The mean solar magnetic field and synoptic frames derived from corrected magnetograms show significant improvement. Standard synoptic charts benefit from reduced noise and elimination of systematic errors in the individual magnetograms. This indicates that this correction is effective and necessary.

1. Introduction

SOHO/MDI measures the line-of-sight velocity, line and continuum intensity, and magnetic field of the Sun (Scherrer *et al.*, 1995). The standard observables are computed from sets of five 1024×1024 filtergrams equally spaced by 75 mÅ near a Ni I spectral line at 6768 Å. The primary observable, Doppler velocity, is derived from four of the filtergrams by calculating a ratio of differences of the intensities and calibrating this ratio to Doppler velocity using an on-board lookup table. The magnetograms are obtained from Doppler shifts measured separately in right and left circularly polarized light (Scherrer *et al.*, 1995).

Uncertainty of the exposure time of the camera shutter induces error in the measurements. The standard deviation of the exposure time of SOHO/MDI is about 12–15 microseconds (Scherrer, 2001, private communication). This means that the sampled intensities are taken with slightly different exposure durations. This shutter noise will add a nearly uniform background offset to each imaged observable.

Such drifts of the zero point exist in other instruments due to various effects. For the magnetograph at Mt. Wilson, Ulrich *et al.* (2002) devised a technique to correct this drift. They first determine the distribution function for the Stokes V signal acquired by their instrument, and then apply an additive adjustment to this signal at each point to shift the peak of the distribution function to zero. Of course, this process will also remove any uniform, genuine solar magnetic field.

Following this technique, in this paper we perform a similar computation to determine the offset in the MDI/SOHO full-disk magnetograms by fitting a Gaus-

Solar Physics **219:** 39–53, 2004.

sian function to the distribution of the low-intensity magnetic field, and show the effect of the 'offset' on the large-scale magnetic field. In Section 2, we describe the method performed. We compare the magnetograms with and without the offset correction in Section 3 and summarize our results in Section 4.

2. Correction of the Offset

The 'offset' in MDI/SOHO magnetograms, described in the previous section, can be corrected under certain assumptions. We note that MDI has an instrumental per pixel magnetic noise level of 20 G for a one-minute observation (Scherrer *et al.*, 1995) and that many pixels in a magnetogram are below this level. If we assume that the noise has a Gaussian distribution and that there is no physical bias on the Sun in the low-flux regions, the shift of the Gaussian center would be the 'offset' caused by the shutter noise. To determine the shift, we first make a histogram of the on-disk pixels of a magnetogram versus magnetic strength; we then fit a Gaussian function to this distribution. The shift of this Gaussian function center is the 'offset' for this magnetogram. Figure 1 gives an example to illustrate how to determine the 'offset'. The diamonds in the upper left panel of Figure 1 form the histogram of the pixels from a selected magnetogram; the thick solid line is the Gaussian function that fits this distribution. The shift of the Gaussian function center is -0.216 G, which we believe to be the magnetic 'offset' for this magnetogram.

We also tried more complex fitting functions, such as two Gaussian functions, three Gaussian functions, and one Gaussian and a polynomial, to better fit the tails of the distribution that reflect contributions of the true magnetic field. The diamonds in the other three panels of Figure 1 are the histograms and the thick solid lines are the final fitted curves. The thin solid line and the dotted line in the right upper panel are the two Gaussian functions that fit the distribution; the dashed, solid, and dotted lines in the lower left show the three Gaussian functions; and the dotted and solid lines in the lower right panel are, respectively, a Gaussian function and a polynomial. The offsets listed in these three cases are the shifts of the Gaussian function that fit the core of the distribution. The offsets are only slightly different.

Another test is done by selecting different parts of the magnetogram and specifying different threshold values above which the pixels are ignored. Figure 2 shows the average value and computed offset versus cutoff threshold in the left panel and the same quantity plotted versus solar radius on the right for a representative magnetogram. B_cutoff in the left panel is the threshold value; Solar Radius in the right panel represents a radius of a circle centered at solar disk center outside of which the pixels are ignored. The solid and dotted lines show variations of the computed offset and average of the magnetic field. The average of the line-of-sight magnetic field is simply computed from the selected pixels. The average varies with B_cutoff and area, but the offset remains nearly constant. This indicates that

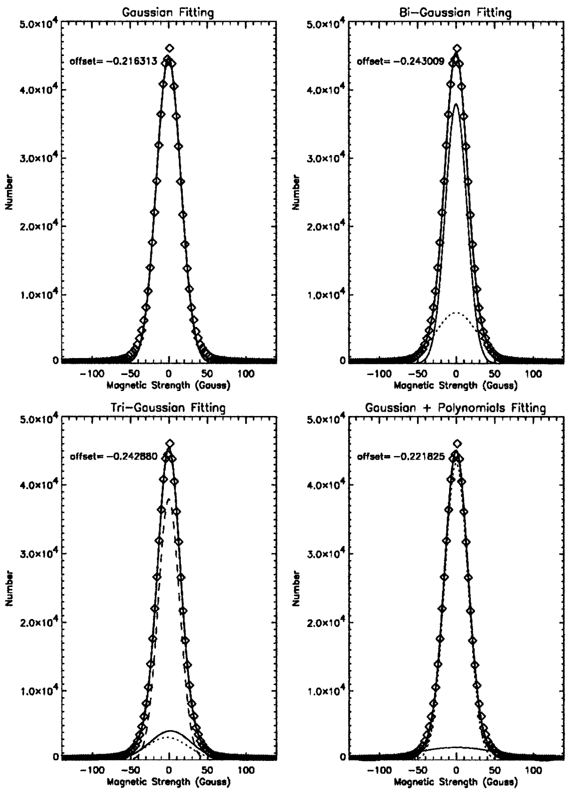

Figure 1. The fitting of distribution of magnetic strength for a magnetogram with various functions. The *diamonds* are a histogram of the on-disk pixels of the magnetogram versus magnetic strength. The *thick solid curves* are the fitting functions. One Gaussian function, two Gaussian functions, three Gaussian functions, and one Gaussian and one polynomial are used separately to fit this distribution, shown in different type lines in *upper left, right* and *lower left* and *right panels*, respectively. The offsets marked in the panels are the shift of the center of the Gaussian function that fits the core of the distribution.

this method is effective and reliable. We use a cut-off value of 300 G and fit out to 95% of the solar radius.

The offset might slightly vary over solar disk. The reasons are that, although the algorithm for computing the MDI Doppler velocity is very insensitive to line depth and to variations in the slopes of the wing intensities, the ratio of differences of the intensities, as a measure of velocity computed from the four filtergrams, doesn't linearly respond to large Doppler shift, and that the shutter's exposure is not uniform across the field of view (Scherrer *et al.*, 1995). The offset near the limb thus may be different from that near the disk center. In order to estimate this difference, we calculated the offsets respectively from the entire solar disk and from the areas near the limb, for the magnetograms in the period from 13 August 1999 to 13 September 1999. The limb areas chosen are the east area from −90° to

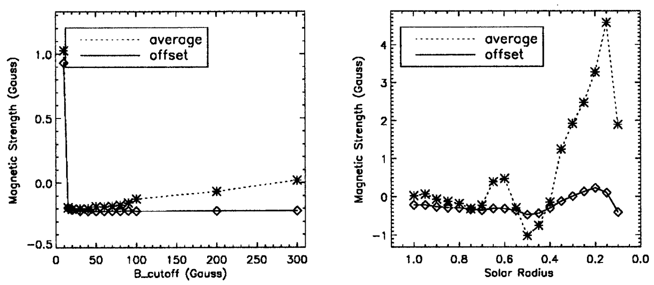

Figure 2. B_cutoff in the *left panel* represents the threshold value above which the pixels are ignored; Solar Radius in the *right panel* is a radius of a circle centered at solar disk center outside of which the pixels are ignored. The *solid and dotted lines* show variations of the calculated offsets and averages of magnetic field. The average of magnetic field here is simply computed from the selected pixels.

$-30°$ in longitude and from $-45°$ to $45°$ in latitude, and the west area from $30°$ to $90°$ in longitude and from $-45°$ to $45°$ in latitude. The difference of the two offsets is about 25% on average. The non-linearity and non-uniformity seem to induce a minor variation of the offset over solar disk. This variation will broaden the width of the Gaussian function used for fitting the distribution of magnetic strength.

Very recently, Berger and Lites (2003) found that the MDI full-disk magnetogram calibration systematically underestimates solar magnetic flux densities relative to the Advanced Stokes Polarimeter (ASP) measurements by a scale factor between 0.64 and 0.71. Since this factor seems to be nearly constant, the impact of this result may be only to increase the values of magnetic field by a constant factor. In this way, the offset is simply multiplied by this constant. We don't apply this correction to MDI data in the rest of this paper.

3. Comparison of Magnetograms with and without the Offset Correction

3.1. Mean Solar Magnetic Field

We first consider the time evolution of the mean magnetic field of the Sun. The mean magnetic field is defined as an average of the fields on the whole visible disk obtained by observing in integrated sunlight (see, e.g., Scherrer, 1973), or in short, the magnetic field of the Sun seen as a star (the Sun-as-a-star field). The mean field is believed to be a weighted average of the line-of-sight component of magnetic field. It can thus be measured from the MDI full-disk magnetograms. Figure 3 shows the mean field and 'offset' in a one-month interval from August 13 to September 14, 1999. The top panel is the mean field derived simply by averaging every pixel in each magnetogram; it shows rapid variations superposed on a longer term trend. The second panel shows the 'offset' computed by Gaussian function fitting, as described in the previous section. The thick line in this panel represents a possible residual solar magnetic signal in the 'offset' derived using a low-pass filter based on a wavelet technique. The wavelet transform used here is based on a Daubechies wavelet filter with 12 wavelet filter coefficients. We filtered the signals longer than three days, simply based on an assumption that there are no instrumental operations periodically in that long time scale. The third panel shows the 'true offset' – a high-pass filtered version of the offset signal. The thick line in the bottom panel is the mean field after correcting for the 'true offset', the thin line is the mean field after correcting for the 'offset' and the stars represent the mean field of the Sun measured at Wilcox Solar Observatory (WSO) at Stanford University. Apparently, the mean field is much smoother after correcting for the 'offset', demonstrating that the noise has been greatly minimized. Both mean fields with the 'offset' correction and the 'true offset' correction match well with WSO observation, but it is difficult to judge which one is better. The shutter noise induces a random error of about 0.31 G on average. It also appears that there may be an one-day phase shift between MDI data and WSO observation in this period. Having checked data for other periods, we found that the phase shift is random. We don't know what causes this one-day offset, but random phase shift for other periods may imply that this one-day offset just happen by chance. Note that the WSO mean field is observed in integrated sunlight and uses a different spectral line (Scherrer *et al.*, 1977), so one would not expect a perfect match with MDI observations, e.g., the intensity weighting is different.

MDI creates two types of magnetograms in its 96-min cadence time series, which are referred as *'one-minute'* and *'five-minute'* magnetograms in this paper. A *one-minute* magnetogram is produced from a set of filtergrams collected during a 30-second interval. A *five-minute* magnetogram is the average of five *one-minute* magnetogram observations obtained during a five-minute interval. This average is computed on board the spacecraft. A Gaussian function fit like the ones described above shows an average width of 16.1 G for *one-minute* magnetograms, which means that the random noise level in a measurement is less than 16.1 G, and 9.7 G for *five-minute* magnetograms. Note that the noise level for *five-minute* magnetograms is higher than expected. To investigate the reason(s) for this abnormal noise level, we generated artificial *five-minute* magnetograms from *one-minute* magnetograms in MDI campaign run during which the MDI magnetograms were taken every minute. These artificial *five-minute* magnetograms are produced by simply adding five successive *one-minute* magnetograms taken in an interval of five minutes, similar to the one taken by MDI. The noise level for these data is 9.2 G on average. It seems that noise in MDI magnetograms is more or less correlative in a certain level.

Figure 4 shows the difference between these two types of magnetogram. The thin lines in the upper three panels connect *one-minute* magnetogram values – the mean field without offset correction (top panel), just the 'true offset' (the second panel), and the mean field corrected for the 'true offset' in the third panel. The diamond symbols indicate the *five-minute* magnetogram values. The bottom panel is the magnetic mean field with the 'true offset' correction for both type mag-

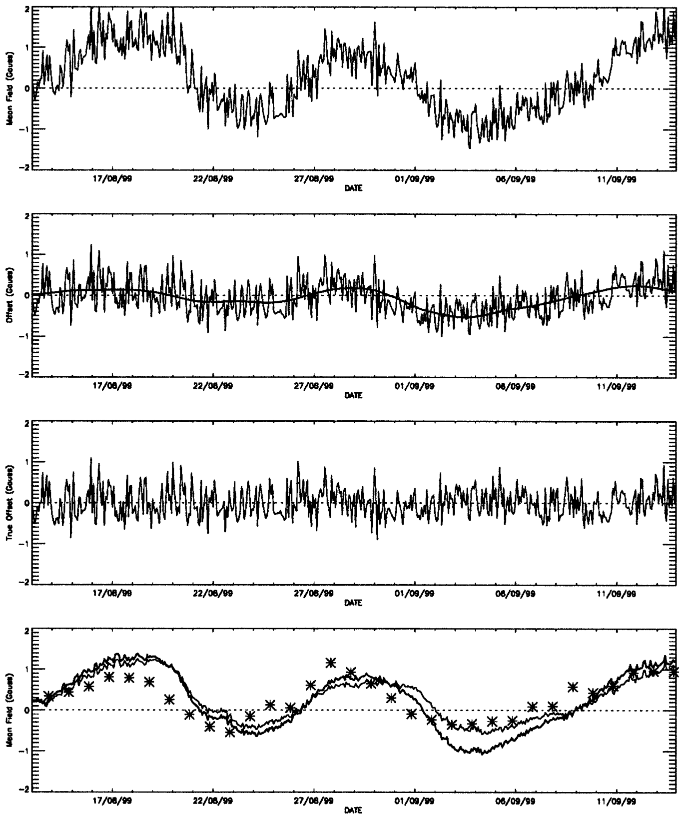

Figure 3. The *top panel* shows the mean field derived simply by averaging every pixel in each magnetogram. The *second panel* is the 'offset' computed by fitting a Gaussian function with distribution of magnetic strength for magnetograms; the *thick line* in this panel represents a possible residual magnetic signal in the 'offset' derived using a wavelet technique. The *third panel* shows the 'true offset' – a high-pass filtered version of the offset signal. The *bottom panel* shows the mean field after correcting for the 'true offset' (*thick line*), for the 'offset' (*thin line*), and the daily mean solar magnetic field measured at the Wilcox Solar Observatory (*stars*). It seems to have an one-day phase shift between the MDI and WSO observations (see text for detail).

netograms. The average and offset of *five-minute* magnetograms are systematically 0.46 G on average lower than those of *one-minute magnetograms*. The additional offset is automatically removed when observables are corrected for the computed offset or the 'true offset'.

So far, we don't know what causes this difference between *one-minute* and *five-minute* magnetograms. It is an obvious systematic error in the observations that probably arises in the on-board data processing. The method used here is able to correct it. This may, in turn, suggest a possible way to inter-calibrate magnetograms acquired by different observatories that possess their own intrinsic errors from instruments, calibrations and data processing. Applying this method to the full-

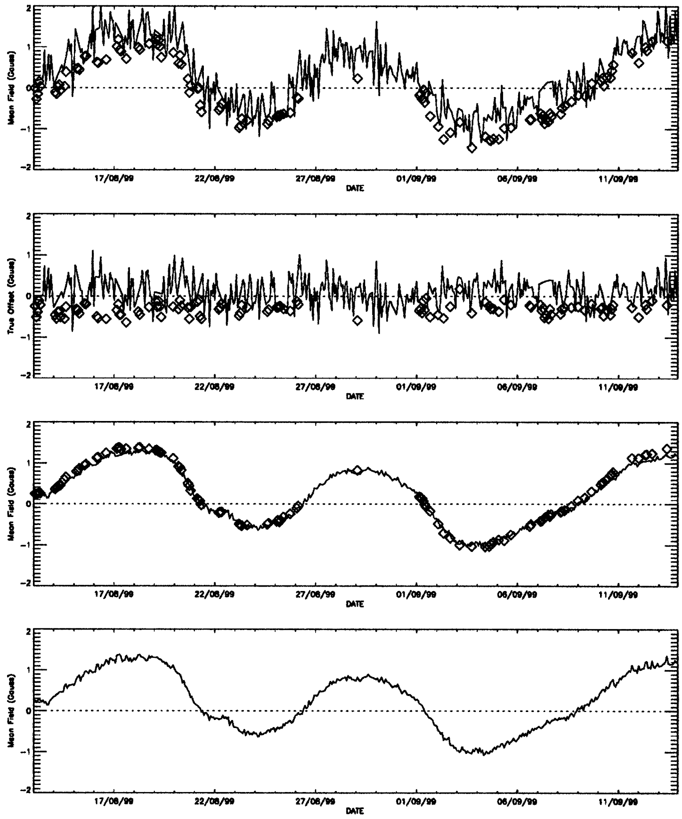

Figure 4. The *thin lines* in the upper three panels represent the magnetic mean field without offset correction (*top panel*), 'true offset' (the *second panel*), and the mean field with 'true offset' corrected (the *third panel*) based on *one-minute* magnetograms; the *diamonds* indicate the *five-minute* magnetogram values. The *bottom panel* is magnetic mean field with the 'true offset' corrected for both types of magnetograms.

disk magnetograms from Kitt Peak, Mt. Wilson, and GONG and comparing them with the MDI/SOHO magnetograms may be of interest. This work is underway.

We have also estimated the magnitude of the yearly median value of the 'offset' correction for *one-minute* magnetograms since the 'offset' for *five-minute* magnetograms itself probably has a systematic error. It is 0.251 G in 1996, 0.268 G in 1997, 0.273 G in 1998, 0.285 G in 1999, 0.391 G in 2000, 0.352 G in 2001, and 0.364 G in 2002. We believe the increase is related primarily to increased noise in the shutter noise and secondarily to solar cycle changes on the Sun.

To estimate the level of the offset solely caused by the shutter noise, we simulated MDI measurement with consideration of this noise. If we assume that the level of jitter in the exposure time is 15 microsecond, a Monte Carlo test gives a median offset of 0.288 G for 1000 experiments. This is consistent with the one from observation.

3.2. Magnetic synoptic charts, frames, and corresponding calculations

Synoptic charts are compiled from multiple magnetograms to build up a map of the entire solar surface. A single point in a standard MDI synoptic chart combines nearly central meridian measurements from approximately 10 individual magnetograms. Variation in the zero level of the observations will contribute to noise in the maps, though at a level much smaller than a typical magnetic feature that has a magnitude of 20 G or more. To test possible influences induced by the offset into other applications, such as synoptic frames and the extrapolation of coronal magnetic structure, we have generated two versions of the magnetic synoptic charts for Carrington rotations (CR) 1919 – CR 1963, February 1997 through May 2000, using MDI data with and without the 'offset' correction. As expected, most charts do not show significant differences because the random offset noise is reduced by the merging. If we assume that the noise for the synoptic charts has a Gaussian distribution, a Gaussian function fitting shows a width of 4.45 G on average for the synoptic charts with the 'offset' correction, 4.46 G for the synoptic charts without the 'offset' correction.

However, we do see obvious differences in CR 1921, CR 1922, and CR 1923. The left panels of Figure 5 are CR 1923 synoptic charts from, respectively, uncorrected MDI magnetograms (the top panel), magnetograms with the 'true offset' correction made (middle), and from the magnetograms taken at WSO (bottom). The white contour lines are the magnetic neutral lines when the spatial resolution of the MDI synoptic charts has been reduced to that of the WSO synoptic chart. The MDI offset-corrected synoptic chart appears to match the WSO synoptic chart better. Note that the MDI charts shown here have been smoothed, reducing the original resolution by a factor of six to a dimension of 360×180; the WSO chart has 72×30 pixels.

Because regions of strong field strength dominate the photospheric field synoptic charts, they are not particularly sensitive to small changes in the background field. Computations of the coronal field, on the other hand, average out all but the largest of structures. Since most of the intense bipolar field cancels, the result is more sensitive to global changes in the zero level. We perform calculations of the potential field to look into the effects of the 'offset'. The right panels of Figure 5 show the locus of the computed heliospheric current sheet and the locations of the foot points of open field lines that correspond to the locations of coronal holes. These are computed from the corresponding synoptic charts at the left using a Potential Field Source Surface model (PFSS) (e.g., Schatten *et al.*, 1969; Altschuler and Newkirk, 1969; or Hoeksema, Wilcox, and Scherrer, 1982). The black lines represent the heliospheric current sheet that separates regions of opposite magnetic polarity; and the dots are the locations of open field line foot points in positive (blue) and negative polarity (red) magnetic polarity regions. The shapes of the current sheet, and the sizes, and patterns of the coronal holes calculated from the

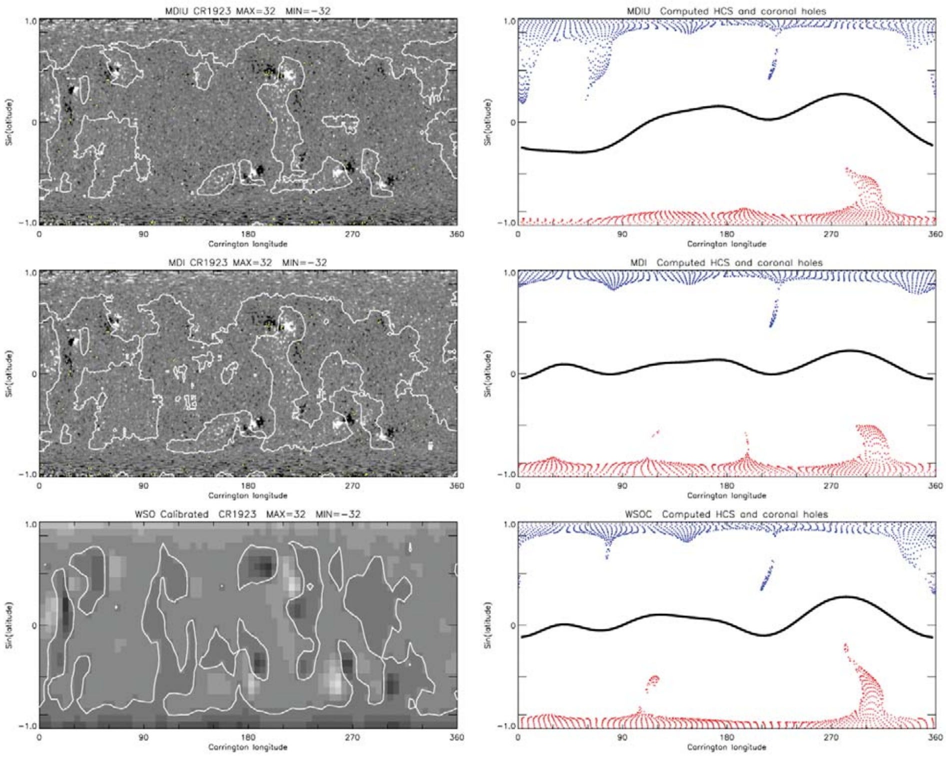

Figure 5. The *left panels* are magnetic synoptic charts generated from MDI magnetograms without the 'offset' correction (*top*), with the 'true offset' correction (*middle*), and from WSO magnetograms (*bottom*), for CR 1923. The *white contour lines* represent magnetic neutral lines when the spatial resolution of MDI data has been reduced to that of WSO data. The *right panels* show the locus (*black lines*) of the computed heliospheric current sheet, the locations of the foot points of the calculated coronal holes (*blue dots* for positive magnetic polarity and *red dots* for negative magnetic polarity). The ticks in these plots represent the latitude of $-60°$, $-30°$, $0°$, $30°$, $60°$.

'corrected' and 'un-corrected' synoptic charts are discernibly different. There is once again a good agreement between the WSO data and the 'corrected' MDI data.

The CR 1921–1923 synoptic charts computed from the 'corrected' and 'un-corrected' magnetograms are significantly different because only *five-minute* magnetograms are available in this interval (see Figure 6). As described in the previous section, the *five-minute* magnetograms values are systematically lower. However, the synoptic charts constructed using offset-corrected magnetograms will have accounted for this and the shutter-noise error. The coronal field calculations are particularly sensitive to this large-scale offset error, as seen in the map of current sheet and coronal hole foot points.

Synoptic charts give a good picture of the solar magnetic field configuration measured over a solar rotation at central meridian. Another type of Carrington synoptic map, the 'synoptic frame' or 'updated synoptic map', provides a tool for

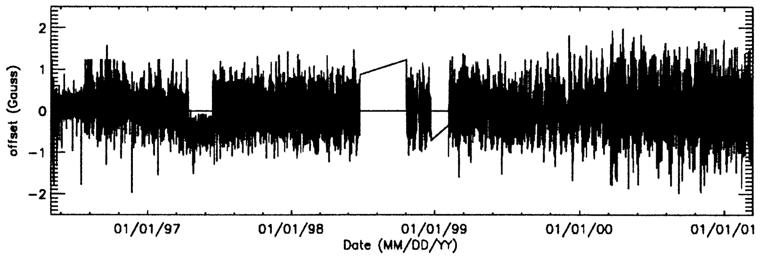

Figure 6. The offsets of MDI magnetograms from 30 April 1996 to 12 March 2001. The offsets systematically lower than zero in the period between March 1997 and June 1997 are calculated from the *five-minute magnetograms* only available then. The gaps at the middle of 1998 and at the beginning of 1999 are due to no operation of SOHO/MDI.

studying the time variation of the photospheric field on the time scale of a day or less (Zhao, Hoeksema, and Scherrer, 1997). A synoptic frame uses data from a single magnetogram taken at the time of interest to replace a portion of the standard synoptic chart. This provides a better estimate of the evolving global magnetic field at a particular instant in time. Not surprisingly, the offset of this magnetogram induces an irregularity in the 'synoptic frame' that affects the calculations.

To illustrate the effects of this error, we choose two *one-minute* MDI magnetograms to generate synoptic frames, one in solar minimum with an 'offset' of 1.31 G recorded at 19:11 UT on 4 October 1997, and the other in solar maximum with an 'offset' of 0.93 G observed at 23:59 UT on 28 January 2001. The top two panels of Figure 7 show these two magnetograms without the 'offset' correction, the middle panels have been corrected for the 'offset', and the bottom panels are the corresponding WSO magnetograms. The contours represent magnetic field in positive polarity (blue), negative polarity (red), and the neutral line (black). In drawing the contours, the spatial resolution of the MDI magnetograms is degraded to the resolution of the WSO magnetograms. The MDI data appear to be improved after correcting the offset: the neutral lines are more similar to those of the WSO data.

Figures 8–9 compare the 4 October 1997 synoptic frames made with the offset correction (top panel of Figure 8) and without the offset correction (top panel of Figure 9); the bottom panels show the radial component of the magnetic field computed at 2.5 solar radii based on the synoptic frames and a PFSS model. The white lines in these figures are magnetic neutral lines. We can see remarkable differences in the synoptic frames as well as in the calculated radial field maps. The offset-corrected synoptic chart matches the calculations based on WSO data better.

Differences are also evident in the synoptic frames and the computed radial field at coronal source surface using the 28 January 2001 magnetogram, which is in the solar maximum phase (see Figures 10–11). The differences near the center of the chart are not as dramatic, perhaps because the overall flux is larger at solar maximum and the structuring is more closely tied to the presence of active regions.

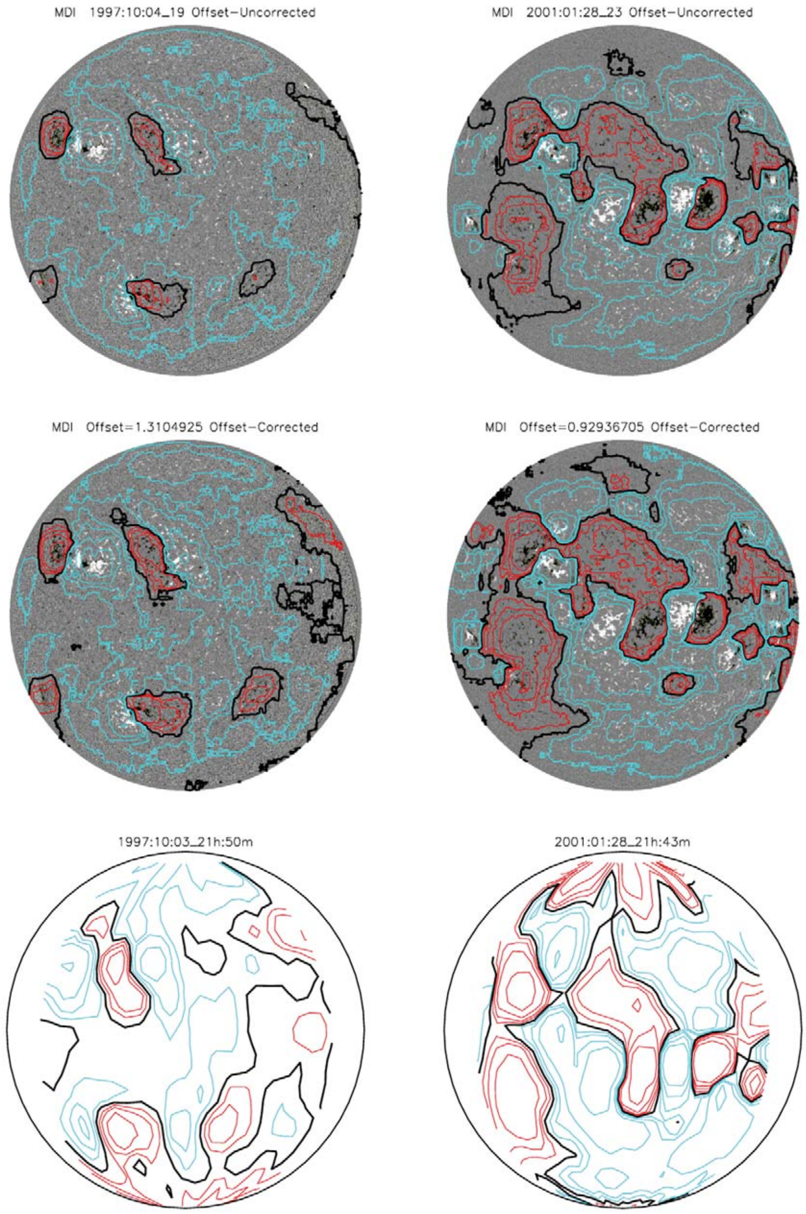

Figure 7. Individual MDI magnetograms without 'offset' correction (*top panels*), with 'offset' correction (*middle panels*), and the corresponding WSO magnetograms (*bottom panels*). These magnetograms were taken in solar minimum (4 October 1997), and in solar maximum (28 January 2001). The color contours represent magnetic field in positive polarity (blue), negative polarity (red), and the magnetic neutral lines (black). These magnetograms are used to create synoptic frames. See the text for more details.

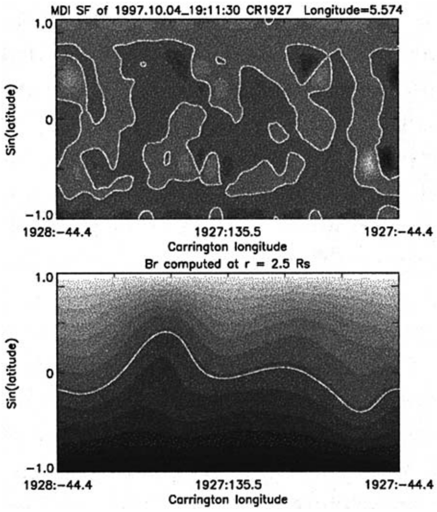

Figure 8. The *top panel* is a synoptic frame using the 4 October 1997 MDI magnetogram shown in Figure 7. The ‘offset’ of this magnetogram is removed. The computed magnetic radial component at 2.5 solar radii are presented in the *bottom panel*. The *white contours* represent magnetic neutral lines. The ticks represent the latitude of $-60°$, $-30°$, $0°$, $30°$, $60°$.

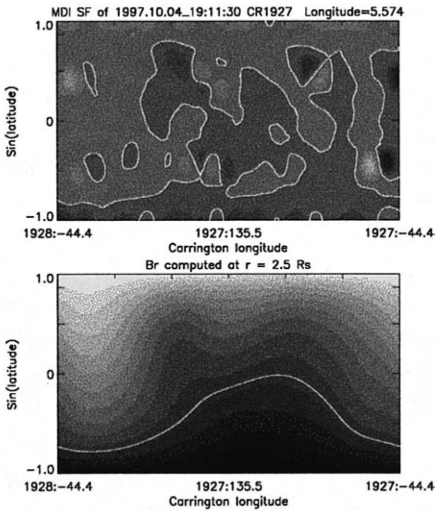

Figure 9. Same as Figure 8, but ‘offset’ is not corrected.

Small offsets in the large-scale field are relatively less important when intense fields dominate the coronal structure. Even so, the detailed location of the neutral line remains sensitive to the zero offset.

Although we have not noticed appreciable differences in the calculated coronal magnetic field from most standard synoptic charts with and without correcting for ‘offset’, we believe that reduction of noise in the charts by virtue of correcting for ‘offset’ may improve other synoptic chart-based applications more sensitive to small variation. Furthermore, the synoptic frames and possible systematic errors in MDI magnetograms have shown potential to induce significant errors in various applications if ‘offset’ is not removed from every individual magnetogram. One important application for synoptic frames, for example, is to predict the polarity of the interplanetary magnetic field and solar wind properties at the Earth for space weather forecasts (see, e.g., Schrijver and DeRosa, 2003).

In summary, correction of the ‘offset’ from MDI magnetograms can greatly improve synoptic frames because the individual magnetograms have a systematic error caused by performance of the instrument; the corrected frames improve the calculations of the coronal field very noticeably because of their sensitivity to large-scale fields. The noise for the standard synoptic charts is slightly reduced, because they are generated by averaging magnetograms. Of course the systematic difference between *one-minute* and *five-minute* magnetograms will be important even for the standard charts.

4. Summary

The shutter noise of the SOHO/MDI instrument induces a small random ‘offset’ into the magnetic measurements. To determine the offset of a particular magnetogram, we fit a Gaussian function to the distribution of the magnetic field values below 300 G. The computed offset is not very sensitive to the cut-off value. The shift of the Gaussian function center is nearly uniform across the disk and has a magnitude of about a third of a gauss. This offset should be subtracted from the entire magnetogram.

We have also discovered a systematic difference between MDI *five-minute* and *one-minute* magnetograms. The cause of this systematic error is uncertain, but is probably related to the on-board processing of the *five-minute* magnetograms. This error is detected and corrected using our offset fitting method.

Some fraction of the physically significant mean magnetic field of the Sun is present in this computed offset. By applying a high-pass filter to a time series of the computed offset, we derive a ‘true offset’ that provides the best estimate of the zero-level error of the MDI magnetograms.

Mean field and synoptic frames computed from corrected magnetograms show significant improvement. These two quantities are particularly sensitive to large-scale offsets in the measured magnetic field strength. This demonstrates that this correction is effective and necessary. This method may also be useful for removing systematic errors in magnetograms from other observatories induced by instruments and/or data processing.

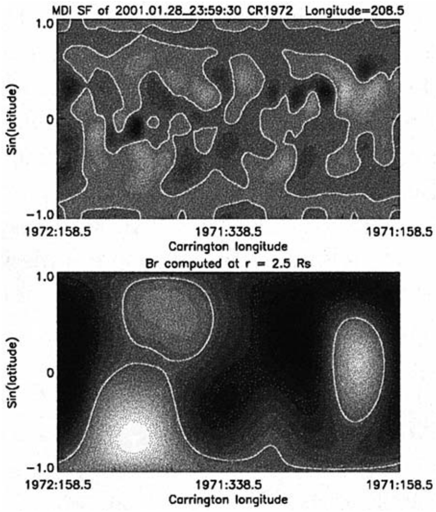

Figure 10. The *top panel* is a synoptic frame using the 28 January 2001 MDI magnetogram shown in Figure 7. The 'offset' of this magnetogram is removed. The computed magnetic radial component at 2.5 solar radii is presented in the *bottom panel*. The *white contours* are magnetic neutral lines. The ticks represent the latitude of −60°, −30°, 0°, 30°, 60°.

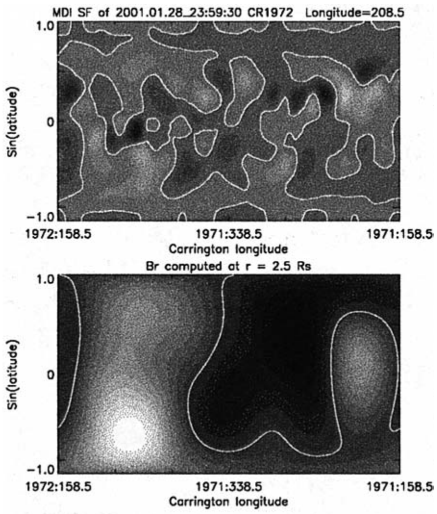

Figure 11. Same as Figure 10, but 'offset' is not corrected.

Acknowledgements

The correction scheme presented in this research builds on a method presented by Roger Ulrich. The constructive comments and suggestions from the anonymous referee, which led to an improvement in this work, are highly appreciated. We thank Phil Scherrer for useful discussions and suggestions. Thanks are also due to

Y. Yan who suggested to use wavelet technique to remove the long-term variation. This work was supported by NASA NAG3-30386. SOHO is a joint project between the European Space Agency and NASA.

References

Altschuler, M. D. and Newkirk, G., 1969, *Solar Phys.* **9**, 131.

Berger, T. E. and Lites, B. W., 2003, *Solar Phys.* **213**, 213.

Hoeksema, J. T., Wilcox, J. M., and Scherrer, P. H.: 1982, *JGR* **87**, 10331.

Schatten, K., Wilcox, J. K., and Ness, N. F.: 1969, *Solar Phys.* **6**, 442.

Scherrer, P. H., Bogart, R. S., Bush, R. I., Hoeksema, J. T., Kosovichev, A. G., Schou, J., Rosenberg, W., Springer, L., Tabell, T. D., Title, A., Wolfson, C. J., Zayer, I. and MDI Engineering Teams: 1995, *Solar Phys.* **162**, 129.

Scherrer, P. H., Wilcox, J. M., Svalgaard, L., Duvall, T. L. Jr., Dittmer, P. H., and Gustafson, E. K.: 1977, *Solar Phys.* **54**, 353.

Scherrer, P. H.: 1973, Ph.D. Thesis, Stanford University.

Schrijver, C. J. and DeRosa, M. L.: 2003, *Solar Phys.* **212**, 165.

Ulrich, R. K., Evans, S., Boyden, J. E., and Webster, L.: 2002, *Astrophys. J. S.* **139**, 259.

Zhao, X. P., Hoeksema, J. T., and Scherrer, P. H., 1997, in the *Proceedings of The Fifth SOHO Workshop at Oslo*, SP-404, p. 751.